AMERICAN ACADEMY OF OPHTHALMOLOGY®

Perilesional Fundus Autofluorescence Patterns Are Not Static: Longitudinal Transitions in Geographic Atrophy and Association with Disease Progression

Alessio Antropoli, MD,[1,2,*] *Francesco Vacirca, MD,*[1,2,*] *Ugo Introini, MD,*[1,2] *Francesco Bandello, MD,*[1,2] *Maurizio Battaglia Parodi, MD,*[1,2,*] *Maria Vittoria Cicinelli, MD*[1,2]

Purpose: To investigate cross-sectional characteristics and longitudinal changes in perilesional fundus autofluorescence (FAF) patterns in geographic atrophy (GA).

Study Design: Retrospective cohort study.

Participants: One hundred forty-three eyes from 99 patients (70 females) with foveal-sparing GA at baseline, of which 106 eyes from 76 patients were eligible for longitudinal analyses.

Methods: Best-corrected visual acuity, FAF, and OCT findings were collected at all visits. Baseline FAF patterns were determined using a 5-item classification, with tracking of longitudinal changes. Changes in GA growth rate following pattern transitions were investigated through linear mixed models.

Main Outcome Measures: Frequency and timing of perilesional FAF pattern transitions, and their association with GA growth rate.

Results: Of the 106 eyes with follow-up, 23 (22%) showed a change in perilesional FAF pattern after a median of 3 years (interquartile range: 1.74–4.10). Square root GA growth rate was 0.40 mm/year (95% confidence interval [CI]: 0.34–0.46; $P < 0.001$), with modestly faster rate in "diffuse nontrickling" compared with "none" eyes (+0.06 mm/year; 95% CI: 0.004–0.12; $P = 0.036$) and slower rate in eyes showing FAF pattern transitions (−0.12 mm/year; 95% CI: −0.19 to −0.05; $P < 0.001$). Baseline lesion size and other FAF patterns were not significantly associated with progression ($P > 0.05$).

Conclusions: Perilesional FAF pattern transitions occur in a subset of GA eyes and are marked by slower progression, underscoring their potential relevance for disease monitoring and clinical trial design.

Financial Disclosure(s): Proprietary or commercial disclosure may be found in the Footnotes and Disclosures at the end of this article. *Ophthalmology Science 2026;6:100995*

Supplemental material available at www.ophthalmologyscience.org.

Geographic atrophy (GA), the advanced form of age-related macular degeneration (AMD), causes progressive, bilateral loss of central vision and represents a major clinical and socioeconomic burden in older adults.[1] Interest in GA has grown further after the approval in the United States of 2 intravitreal complement inhibitors, pegcetacoplan (Syfovre, Apellis Pharmaceuticals) and avacincaptad pegol (Izervay, Astellas Pharma Inc), which target complement components C3 and C5, respectively.[2–4] These agents have demonstrated efficacy in slowing lesion enlargement, yet neither has been approved in Europe, where the European Medicines Agency raised concerns regarding limited functional benefit in relation to treatment burden.[5] This regulatory stance has reignited interest in identifying imaging biomarkers that may predict faster GA enlargement, to improve patient selection in clinical practice and trials. Among these, perilesional fundus autofluorescence (FAF) patterns have been extensively used as prognostic indicators of GA expansion rate.[6–11] The classification system introduced by Bindewald et al[12] and refined by Holz et al[8] includes "none," "focal," "patchy," "banded," and several "diffuse" configurations. While adopted in multiple trials and cohort studies, this scheme has faced criticism for limited reproducibility and phenotypic overlap with other macular dystrophies, including extensive macular atrophy with pseudodrusen-like appearance (EMAP), leading to the exclusion of certain patterns in later analyses.[9,13–16] To address these challenges, the GAIN study applied clustering algorithms to derive a simplified FAF classification that retained prognostic value while improving intergrader consistency.[17–20] GAIN confirmed strong associations between FAF pattern and baseline GA area, supporting the view that FAF

https://doi.org/10.1016/j.xops.2025.100995
ISSN 2666-9145/25

phenotypes represent a disease continuum rather than discrete entities. However, its relatively short follow-up (FU) (18 months) likely limited the ability to detect longitudinal changes in phenotype.[17]

An alternative quantitative approach introduced by Bearelly et al, rim area focal hyperautofluorescence, calculates the proportion of increased autofluorescence within a 500-μm ring surrounding GA.[21] Rim area focal hyperautofluorescence was shown to correlate with baseline GA size and progression, supporting the notion that FAF changes evolve dynamically.[22,23] Yet, despite these quantitative insights, no study has formally assessed the temporal stability of qualitative FAF patterns. This gap is particularly relevant because major interventional trials, such as GATHER-1, GATHER-2, OAKS, and DERBY, have used baseline FAF phenotype as an inclusion or stratification variable, implicitly assuming that these phenotypes remain stable over time.[2,24] If this assumption is incorrect, it may compromise both patient selection and interpretation of treatment effects in clinical trials.

Against this background, we conducted a longitudinal study focusing on eyes with foveal-sparing GA, a stage often prioritized in clinical trials to maximize the window for therapeutic benefit. We sought to determine whether perilesional FAF patterns evolve over time and whether such transitions are associated with changes in GA enlargement rate.

By evaluating the temporal dynamics of FAF morphology, we aim to provide new insights into GA progression and inform strategies for clinical management, patient stratification, and trial design.

Methods

Study Participants and Enrollment Criteria

This was a retrospective longitudinal study conducted at the IRCCS San Raffaele Scientific Institute (Milan, Italy). Analyses were conducted on a previously published data set examining foveal involvement in GA secondary to AMD, using data collected between April 2011 and November 2023, a timeframe during which all patients were imaged with the same OCT device and scanning protocol.[25] The study protocol adhered to the Declaration of Helsinki and was exempted by the San Raffaele Hospital Institutional Review Board from the requirement for written informed consent. Eligible patients were aged ≥50 years with nonexudative AMD and foveal-sparing GA at baseline, a minimum FU of 6 months, and ≥2 high-quality FAF images. Foveal sparing was defined as the presence of a continuous residual foveal island spanning ≥270° of preserved tissue around the foveal center.[25] Both eyes were included if they met the eligibility criteria. Eyes were excluded if there was any evidence of macular neovascularization during FU, any other coexisting retinal disease, presence of GA due to a cause other than AMD, or prior ocular treatment that could influence GA progression.

Data Collection and Imaging Protocol

All patients underwent standardized ophthalmic assessments, including best-corrected visual acuity (BCVA), blue-light FAF imaging (488 nm), and spectral-domain OCT at all visits. Fundus autofluorescence images were acquired using a confocal scanning laser ophthalmoscope (Spectralis, Heidelberg Engineering) with a 30° × 30° field of view. Spectral-domain OCT was performed using a 20° × 20° volume scan protocol (25 horizontal B-scans, 240 μm spacing, automatic real-time averaging activated).

Baseline FAF images were graded independently by 2 masked readers (A.A. and F.V.). Initially, perilesional FAF patterns were classified using the 9-pattern "specific" scheme proposed by Holz et al,[8] which includes: none, focal, patchy, banded, and 5 subtypes of diffuse patterns (reticular, branching, fine-granular, trickling, and fine-granular with peripheral punctate spots [GPS]). Eyes exhibiting GPS were excluded due to phenotypic overlap with adult-onset Stargardt disease.[14] Eyes with patchy FAF were also excluded, as this category was absent in the simplified classification by Biarnés et al[18] and was represented by only 1 eye in our cohort.

The remaining eyes were reclassified using a modified 5-pattern "general" scheme as: none, focal, banded, diffuse non-trickling, and diffuse-trickling.[18] Eyes showing diffuse-trickling FAF were excluded from longitudinal analysis, due to phenotypic overlap with EMAP.[26] Grading discrepancies were resolved by consensus, and ungradable images were excluded.

All FU FAF images were reviewed by 1 author (F.V.) to identify changes in FAF pattern over time. Any flagged transitions were independently re-evaluated by a second author (A.A.), and an agreement on the occurrence of the transition was reached in every case. The date of the first visit at which both graders concurred that the FAF pattern change was visible was then recorded, and the interval from baseline was calculated.

Additionally, an exploratory analysis was performed on eyes exhibiting FAF pattern transitions, assessing OCT features within 100 μm of the nasal or temporal atrophic border on representative horizontal B-scans intersecting evolving FAF regions, with grading for retinal pigment epithelium (RPE) thickening, ellipsoid zone disruption, and external limiting membrane disruption as detailed in the Supplementary Methods (available at www.ophthalmologyscience.org).

The GA area was manually delineated on FAF images using the "Region Finder" tool in the Heidelberg Eye Explorer software at baseline, last FU, and at the visit when a pattern transition was first identified (if applicable).[25] When atrophy extended beyond the 30° × 30° image frame, the entire visible lesion was measured.

Study Outcomes

The primary outcome was the occurrence of perilesional FAF pattern transitions over time and their association with differences in GA lesion growth rate. The secondary outcomes included the frequency and timing of perilesional FAF pattern changes, baseline GA area stratified by FAF pattern, and the structural OCT features observed at the junctional zone before and after pattern transition.

Statistical Analyses

Continuous variables were summarized as mean ± standard deviation or median with interquartile range (IQR), depending on their distribution. Categorical variables were reported as frequencies and percentages. Intergrader agreement for perilesional FAF pattern classification was assessed using unweighted Cohen kappa statistic (κ).

Differences in baseline GA area among perilesional FAF patterns were assessed using a linear mixed model with FAF pattern as a fixed effect. Longitudinal changes in GA area were modeled with a second linear mixed model, using square root−transformed GA area as the dependent variable. Fixed effects included FU time, baseline square root−transformed GA area, baseline FAF

pattern, and posttransition status. The latter was a binary variable set to 0 before any observed change in FAF pattern and 1 from the first visit showing a transition onward. Interaction terms between FU time and each fixed effect were included to reflect biological plausibility and control for potential confounding. Best-corrected visual acuity was modeled analogously, with fixed effects for FAF pattern, FU time, and their interaction. All models included a random intercept for patient identification to account for intereye correlation and repeated measures. Model diagnostics confirmed adequate fit, with approximately normal residuals, no heteroscedasticity, and no multicollinearity. All statistical analyses were performed using R software (R Foundation for Statistical Computing), and a P value <0.05 was considered statistically significant.

Results

Study Cohort and Baseline FAF Grading

A total of 167 eyes from 115 patients with foveal-sparing GA were initially identified. After exclusions, the final cross-sectional cohort consisted of 143 eyes from 99 patients (Fig 1). Fundus autofluorescence patterns were graded using the original 9-pattern classification,[8] then recoded into a simplified 5-pattern scheme for analysis (Table 1). Intergrader agreement for the 5-pattern system was substantial (Cohen kappa = 0.77; $P < 0.001$). Consensus could not be reached in 3 of 31 discordant cases, which were excluded along with 1 additional eye exhibiting a "patchy" FAF pattern. The final cohort for cross-sectional analysis comprised 143 eyes from 99 patients.

The baseline population included 70 females (71%), and patients had a mean age of 75.1 ± 9.8 years and a median GA area of 2.33 mm^2 (IQR: 0.48−6.04; range: 0.05−29.9) (Table 2). The GA area differed significantly across the 5 perilesional FAF patterns (Table S3, available at www.ophthalmologyscience.org), with the diffuse-trickling exhibiting the largest area, followed by banded, diffuse nontrickling, focal, and none (Fig 2B).

Longitudinal Analyses

Across the 106 eyes included in the longitudinal cohort, a total of 620 FU visits were analyzed. Each eye had a median of 5 visits (IQR: 3−9), spaced a median of 5.1 months apart (IQR: 2.7−7.8), over a median FU of 3.4 years (IQR: 2.1−4.7).

During FU, 23 of 106 eyes (22%) from 21 patients exhibited a transition in perilesional FAF pattern (Fig 3). No eye experienced >1 transition. Pattern changes were most frequent among eyes with a "none" pattern at baseline (11/22; 50%), which predominantly evolved into diffuse nontrickling (n = 10) or focal (n = 1). Among the eyes with focal perilesional FAF at baseline (n = 7), 3 (43%) progressed to diffuse nontrickling. Of the 65 eyes with diffuse baseline patterns, 9 (14%) transitioned to banded. None of the 16 eyes with a baseline banded pattern underwent a transition during FU (Table S4, available at www.ophthalmologyscience.org).

Transitions occurred after a median of 3 years (IQR: 1.7−4.1), at a mean GA area of 5.12 mm^2 (IQR: 3.23−9.42). In 6 cases, the perilesional FAF pattern change was first identified at the final visit. Timing and lesion size at the point of transition varied across baseline FAF pattern, with the largest areas observed in eyes transitioning from diffuse nontrickling (Table 2).

OCT Assessment

Between baseline and the time of FAF pattern transition, 13 of 23 eyes (56.5%) demonstrated horizontal GA enlargement >100 μm, enabling paired structural OCT assessment of both the original and newly exposed perilesional zones. The median margin displacement was 290 μm (IQR: 228−728). In the remaining 10 eyes, lesion margins remained stable, and OCT evaluation was performed at the same location across all visits.

Structural OCT analysis showed that perilesional zones frequently exhibited photoreceptor and RPE alterations both at baseline and at the time of perilesional FAF pattern transition. In contrast, newly formed margins were sometimes structurally preserved at baseline. Detailed descriptions of perilesional changes across different FAF transitions are provided in the Supplementary Results (available at www.ophthalmologyscience.org).

Rate of GA Enlargement

Longitudinal mixed-effects modeling revealed a significant increase in square root−transformed GA area over time, with an estimated annual progression rate of 0.40 mm/year (95% confidence interval [CI]: 0.34−0.46; $P < 0.001$).

Baseline lesion size did not influence the progression rate (interaction $P = 0.6$), and no significant differences were found for eyes with focal ($P = 0.1$) or banded ($P = 0.7$) FAF patterns compared with the "none" reference group. However, eyes with baseline diffuse nontrickling FAF pattern showed a modest but significant increase in progression rate (+0.06 mm/year; 95% CI: 0.004−0.12; $P = 0.04$).

Interestingly, eyes that experienced a transition in FAF pattern during FU exhibited a slower rate of GA enlargement overall (−0.12 mm/year; 95% CI: −0.19 to −0.05; $P < 0.001$), based on analysis comparing baseline, transition, and last available visits (Table 5).

The most pronounced reduction in progression rate was observed in eyes transitioning from "none" to diffuse patterns (−0.31 mm/year), followed by transitions from diffuse to banded (−0.17 mm/year). In contrast, the 2 eyes that changed from focal to diffuse patterns demonstrated a slight acceleration in GA growth (+0.11 mm/year). The progression rate could not be calculated for the single eye transitioning from none to focal, as the change was first detected at the last available visit (Fig 4).

Rate of BCVA Decline

At baseline, the median BCVA across the cohort was 0.25 logarithm of the minimum angle of resolution (IQR: 0.1−0.4), with eyes in the banded group showing the worst visual acuity of 0.4 logarithm of the minimum

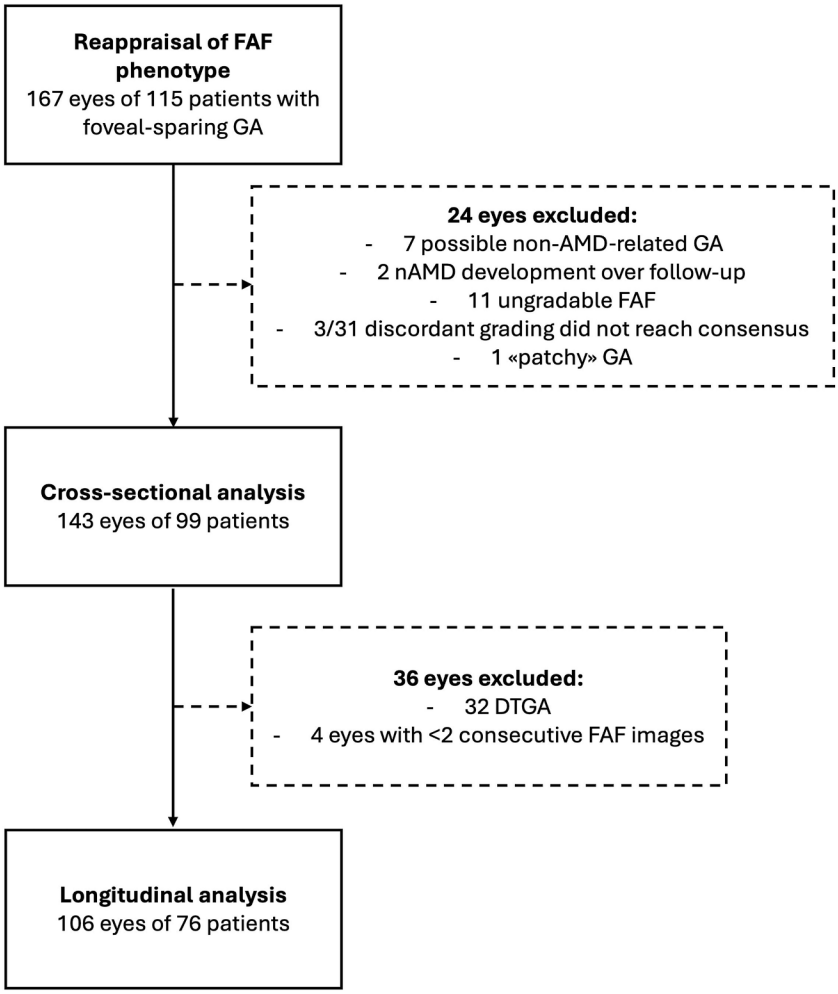

Figure 1. STROBE diagram illustrating patient and eye exclusions leading to the final cross-sectional and longitudinal cohorts. AMD = age-related macular degeneration; DTGA = diffuse-trickling geographic atrophy; FAF = fundus autofluorescence; GA = geographic atrophy; nAMD = neovascular age-related macular degeneration.

angle of resolution (IQR: 0.3−0.7). Conversely, no differences in the rate of BCVA decline were detected across FAF patterns (all $P > 0.05$) (Table S6, available at www.ophthalmologyscience.org). A simpler model pooling across FAF patterns estimated a statistically significant worsening in BCVA over time ($\beta = 0.056$ logarithm of the minimum angle of resolution/year, 95% CI: 0.033−0.078; $P < 0.001$), corresponding to an average loss of approximately half a Snellen line lost per year.

Discussion

In this longitudinal study of foveal-sparing GA eyes due to nonexudative AMD, we examined whether perilesional FAF patterns change over time, and characterized the timing, frequency, and structural correlates of such transitions, along with their relationship to baseline atrophy size and lesion growth rate.

Three key findings emerged. First, baseline FAF phenotype was significantly associated with GA area, with diffuse-trickling and banded patterns linked to more extensive atrophy, consistent with prior cross-sectional studies.[17] Second, worse baseline BCVA was observed in eyes with a banded pattern, although FAF phenotype was not associated with the rate of visual decline, suggesting limited prognostic value for this functional endpoint. Third, FAF patterns were dynamic: approximately 22% of eyes showed a phenotypic transition during FU, most often from "none" or "focal" to "diffuse nontrickling" or "banded" patterns. Taken together, these observations support a staged model of perilesional FAF evolution, in which the perilesional hyper-FAF area changes over time,[22] and eyes progress from no detectable junctional hyperautofluorescence to focal patterns, followed by diffuse nontrickling, and finally to the banded configuration (Fig 5). This dynamic remodeling challenges the notion of static FAF phenotypes and underscores the need for longitudinal

Table 1. Baseline Grading Results

	Grader 1	Grader 2	Final Grading
9-Item Classification (Adapted from Holz et al)			
None	21 (14.3)	28 (19.0)	22 (15.3)
Focal	9 (6.1)	12 (8.2)	7 (4.9)
Patchy	2 (1.4)	1 (0.7)	1 (0.7)
Banded	16 (10.9)	16 (10.9)	18 (12.2)
Diffuse*			
Reticular	57 (38.8)	56 (38.1)	55 (37.4)
Branching	9 (6.1)	4 (2.7)	8 (5.5)
Granular	2 (1.4)	0 (0)	1 (0.7)
Trickling	31 (21.1)	30 (20.4)	32 (22.2)
5-Item "General" Classification (Modified from Biarnés et al)			
None	20 (13.9)	27 (18.9)	22 (15.4)
Focal	9 (6.3)	11 (7.7)	7 (4.9)
Banded	16 (11.2)	16 (11.2)	18 (12.6)
Diffuse			
Nontrickling	67 (46.9)	59 (41.2)	64 (44.8)
Trickling	31 (21.7)	30 (21.0)	32 (22.4)

Final grading for the 9-item classification only included 144/147 eyes due to lack of consensus between the graders and 143 eyes in the 5-item "general" classification due to further exclusion of 1 "patchy" eye.
*The "diffuse fine-granular with peripheral punctate spots (GPS)" was not included due to phenotypic overlap with *ABCA4*-related retinopathy. The prevalence of different patterns is expressed as number (%).

Table 2. Cross-Sectional Cohort Demographics and FAF Pattern Transition Data

Cross-Sectional (N = 143 Eyes from 99 pts)		
Females, n		70
Age (yrs), mean ± SD		75.1 ± 9.8
GA Area at Baseline*	**Original (mm^2), Median (IQR)**	**Square Root Transformed (mm), Median (IQR)**
Whole cohort (143 eyes)	2.33 (0.48–6.04)	1.53 (0.69–2.46)
FAF pattern: none (22)	0.48 (0.31–0.79)	0.69 (0.55–0.89)
FAF pattern: focal (7)	1.00 (0.25–1.67)	1.00 (0.49–1.28)
FAF pattern: diffuse nontrickling (64)	1.31 (0.40–3.87)	1.14 (0.63–1.97)
FAF pattern: diffuse-trickling (32)	8.51 (4.5–10.7)	2.92 (2.12–3.27)
FAF pattern: banded (18)	5.76 (3.76–8.56)	2.40 (1.94–2.93)
Longitudinal (N = 106 Eyes from 76 pts)		
Observed pattern transitions, eyes (pts)		23 (21)
Time elapsed before transition (yrs), median (IQR)		
Overall		2.97 (1.74–4.1)
FAF pattern: none (11)		2.77 (1.81–3.50)
FAF pattern: focal (3)		1.36 (1.33–3.25)
FAF pattern: diffuse nontrickling (9)		3.24 (2.97–4.22)
GA Area at the Moment of Transition	**Original (mm^2), Median (IQR)**	**Square Root Transformed (mm), Median (IQR)**
Overall	5.12 (3.23–9.42)	2.26 (1.79–3.07)
FAF pattern: none (11)	4.99 (2.46–6.36)	2.23 (1.57–2.51)
FAF pattern: focal (3)	2.84 (2.66–3.58)	1.69 (1.63–1.88)
FAF pattern: diffuse nontrickling (9)	9.37 (6.77–16.9)	3.06 (2.60–4.11)

FAF = fundus autofluorescence; GA = geographic atrophy; IQR = interquartile range; SD = standard deviation.
*Baseline FAF patterns following the 5-item "general" classification.

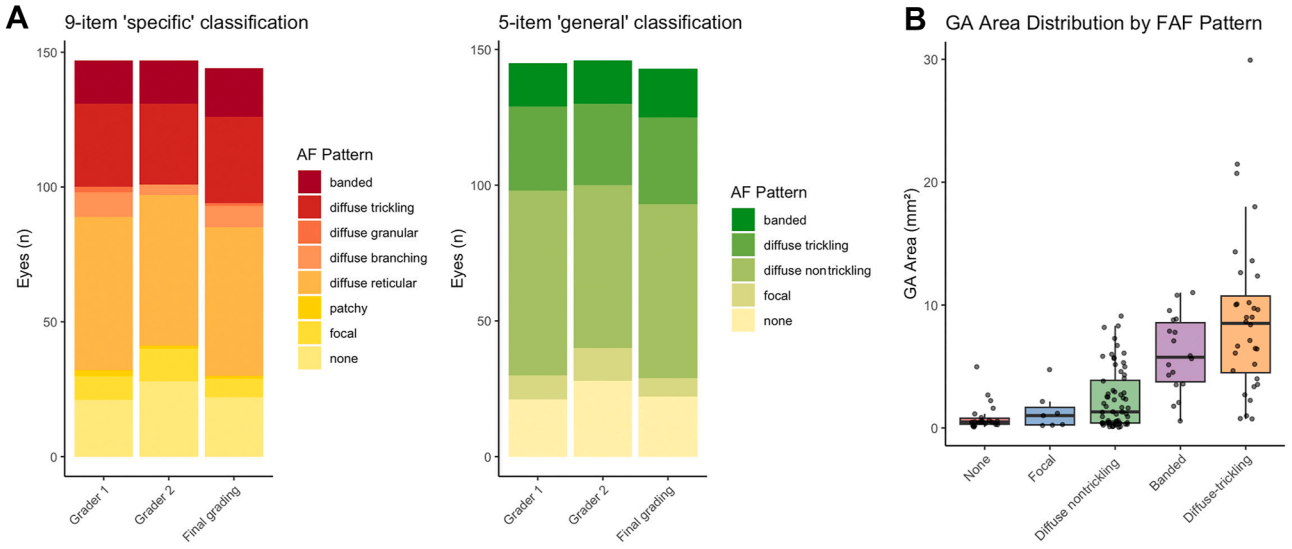

Figure 2. **A,** Baseline FAF grading results with the 9-item (left) and 5-item (right) classifications. Note the "diffuse-GPS pattern" was removed from the "specific" classification due to phenotypic overlap with Stargardt disease. **B,** Boxplots showcasing the distribution of GA area by FAF pattern according to the "general" classification. AF = autofluorescence; FAF = fundus autofluorescence; GA = geographic atrophy; GPS = fine-granular with peripheral punctate spots.

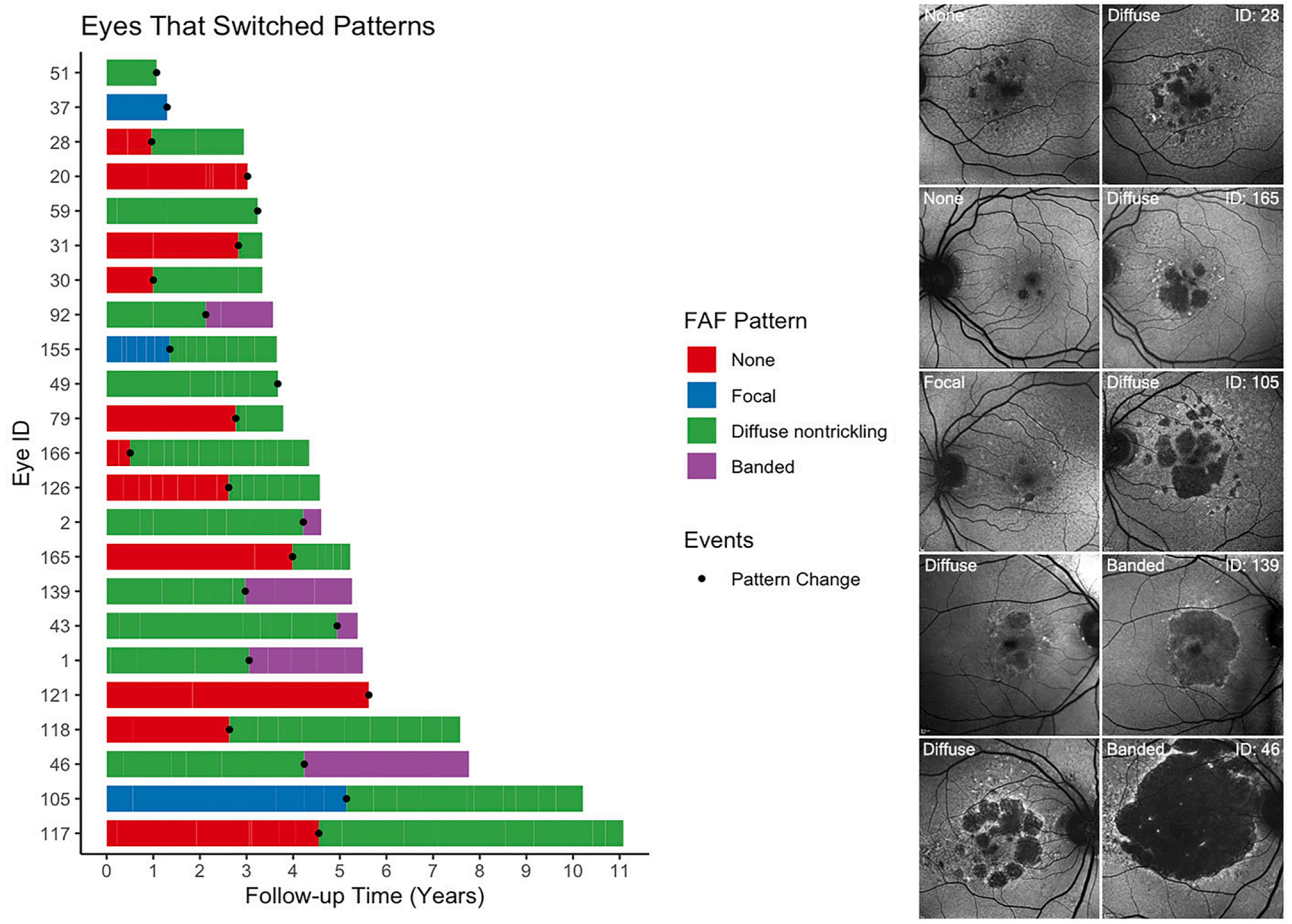

Figure 3. Swimmer plot of eyes that transitioned to a different FAF pattern over time. Each bar represents an eye's follow-up, with colors indicating the FAF pattern at each visit. White vertical lines mark follow-up visits, and black dots indicate visits where a pattern change was detected. Representative FAF images show baseline patterns (left) and their changes over time (right). FAF = fundus autofluorescence; ID = identification.

Table 5. Factors Influencing Square Root GA Area Change Over Time

	Estimate	95% CI	*P* Value
FU time (yrs)	0.4	(0.34, 0.46)	**<2e^{-16}**
FU time × BL square root of GA area (mm)	−0.01	(−0.04, 0.02)	0.606
FU time × BL FAF pattern: none (*ref.*)			
FU time × BL FAF pattern: focal	−0.06	(−0.14, 0.02)	0.138
FU time × BL FAF pattern: diffuse nontrickling	0.06	(0.004, 0.12)	**0.036**
FU time × BL FAF pattern: banded	−0.02	(−0.13, 0.09)	0.699
FU time × postpattern transition	−0.12	(−0.19, −0.05)	**0.0005**

BL = baseline; CI = confidence interval; FAF = fundus autofluorescence; FU = follow-up; GA = geographic atrophy.
Dependent variable = square root of GA area (mm). Data were nested between patients. Number of observations (patients) = 235 (76). Statistically significant *P* values in bold.

evaluation when interpreting perilesional FAF morphology in GA.

These observations build upon the hypothesis proposed in the GAIN study, which established a cross-sectional association between perilesional FAF pattern and baseline GA area, and introduced a simplified classification to improve reproducibility.[17] However, GAIN's limited 18-month FU likely precluded detection of longitudinal transitions. Our findings extend this model by demonstrating that FAF patterns can evolve longitudinally, typically at intermediate lesion sizes and later disease stages, underscoring the importance of temporal context when interpreting perilesional FAF features. Notably, we did not observe any eye undergoing multiple FAF pattern transitions, possibly because sequential shifts require longer periods than our FU allowed, or because certain configurations, such as the banded pattern, may represent a more stable end-stage phenotype with limited capacity for further qualitative change.

Additional insight into the structural basis of FAF pattern evolution was provided by exploratory OCT analysis, which revealed that structural alterations at the perilesional zone were common before FAF pattern transitions, though not uniformly present. Ellipsoid zone disruption was the most consistent finding at baseline across groups, while ELM disruption and RPE thickening varied depending on the transition type. An increase in RPE thickening was noted particularly in eyes evolving to the diffuse nontrickling pattern, suggesting some structural remodeling over time. Nonetheless, several eyes with measurable GA margin displacement showed no structural abnormalities in the newly exposed perilesional areas on baseline OCT, suggesting a disconnection between visible structural damage and future atrophic expansion. These findings suggest that OCT-based markers may capture some aspects of local vulnerability but may not detect earlier molecular or subclinical changes that precede morphological degeneration. Given that our assessment was limited to a single representative margin per eye, these observations should be viewed as hypothesis-generating rather than exhaustive.

In our cohort, the mean square root−transformed GA growth rate was 0.4 mm/year, consistent with the sham arms of major clinical trials testing complement inhibitors.[3,27] Among baseline phenotypes, diffuse nontrickling FAF was the only pattern associated with significantly faster GA enlargement. In contrast, other configurations, including banded and focal, showed no significant differences in growth rate compared with the reference group, likely reflecting the nonlinear nature of GA progression.[28] Importantly, these anatomical

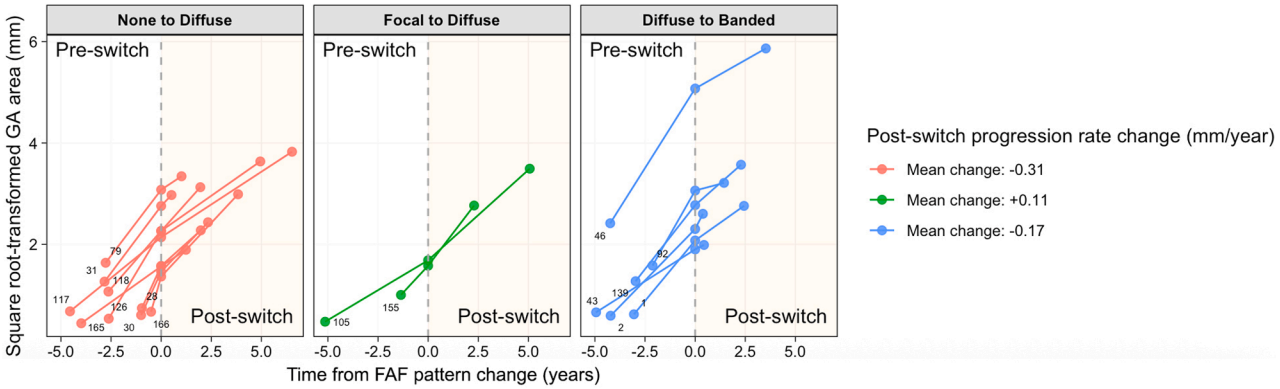

Figure 4. Change in GA enlargement rate after FAF pattern transitions. Each panel displays the square root−transformed GA area (mm) over time for eyes that underwent a transition between FAF patterns. The vertical dashed line marks the time of pattern change, separating preswitch and postswitch phases. Numbers indicate individual eye IDs, connected by lines and color-coded by transition type. The mean postswitch changes in GA progression rate (mm/year) are shown on the right, demonstrating a slowdown after none-to-diffuse and diffuse-to-banded transitions, and a slight acceleration after focal-to-diffuse. FAF = fundus autofluorescence; GA = geographic atrophy; ID = identification.

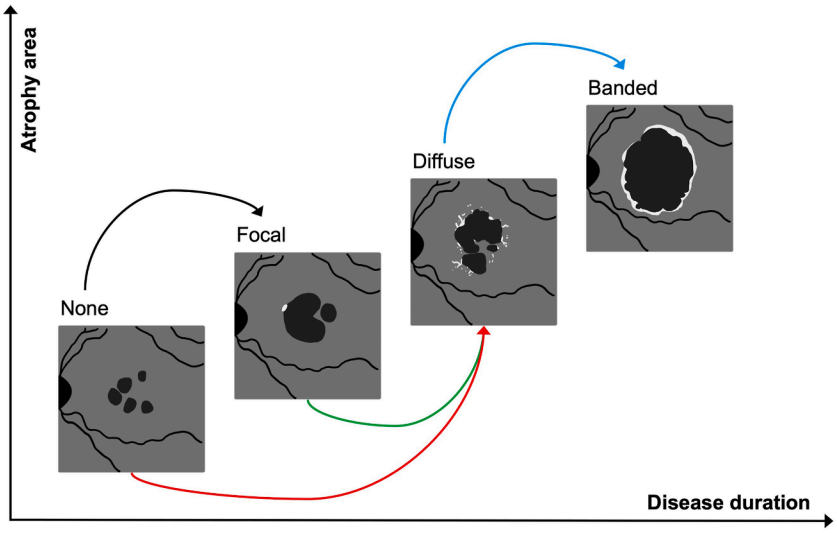

Figure 5. Proposed scheme of perilesional FAF pattern evolution in GA. Arrows indicate the directions of transitions that were documented in this cohort. Most eyes evolved from none or focal to diffuse nontrickling patterns and from diffuse nontrickling to banded configurations. In contrast, banded patterns remained stable throughout follow-up, likely representing the natural endpoint of FAF evolution. Consistent with this sequence, none and focal patterns were typically observed in eyes with smaller GA areas, diffuse nontrickling patterns in eyes with small-to-intermediate lesions, and banded patterns in eyes with the largest atrophic areas. We propose that FAF pattern transitions occur as macular atrophy enlarges and reaches the typical GA size range associated with the next perilesional FAF configuration. FAF = fundus autofluorescence; GA = geographic atrophy.

differences did not translate into variations in the rate of visual acuity decline, further reinforcing the notion that perilesional FAF morphology alone may have limited prognostic value for functional outcomes in foveal-sparing GA.

One of the more unexpected findings in our study was that eyes undergoing a perilesional FAF pattern transition demonstrated a slower rate of GA enlargement. This was particularly surprising given that diffuse nontrickling, a common transition endpoint, was the only baseline phenotype associated with faster GA progression. This apparent paradox may be explained by the timing and context in which transitions occurred: many occurred at later FU visits, when lesion growth is known to decelerate as GA area increases.[29] Alternatively, it is plausible that slower lesion expansion permits more time for perilesional structural remodeling, making FAF transitions easier to detect. The observed interaction between FU duration and transition status thus suggests that FAF evolution is more likely to be captured in eyes with slower disease trajectories.

Notably, growth rate in transitioning eyes was calculated using only the time points from baseline to the transition visit and from transition to final FU, not across all available visits. While this strategy aligns growth dynamics with the timing of phenotypic change, it may underestimate more subtle, continuous fluctuations in lesion progression. Future studies with denser imaging intervals and spline-based modeling may help clarify the temporal relationship between structural remodeling and phenotypic shifts. The findings from this study have direct relevance to clinical trial design. Several phase III studies evaluating complement inhibition, such as GATHER-2, OAKS, and DERBY, incorporated baseline perilesional FAF phenotypes into eligibility or randomization criteria. In OAKS and DERBY, evaluating pegcetacoplan, eyes with a "none" pattern were excluded, while GATHER-2, evaluating avacincaptad pegol, stratified participants by randomizing those with "none" or "focal" patterns separately from those with "diffuse" or "banded" configurations.[2,3] CHROMA and SPECTRI, the lampalizumab trials, applied similar requirements by limiting inclusion to eyes with diffuse or banded phenotypes.[27] While these strategies aim to enrich for faster progressors and ensure cohort homogeneity, they rest on the assumption that perilesional FAF phenotype remains stable throughout the study period, a premise our data challenge. If FAF patterns evolve, then fixed baseline classification may mischaracterize disease trajectories and obscure differential treatment responses.

Further complicating this landscape is the known phenotypic overlap between certain FAF patterns and inherited macular dystrophies. For instance, the "diffuse GPS" pattern has been later reclassified as Stargardt disease, while the "diffuse granular" phenotype has shown strong similarity to *PRPH2*-related central areolar choroidal dystrophy.[13,14] More recently, our group and others have proposed that the so-called "diffuse-trickling" pattern, often considered the most aggressive GA phenotype, may frequently correspond to EMAP, a distinct entity with specific demographic, clinical, and imaging features.[15,16,26,30–32] This is especially relevant in the context of GATHER-1, which included up to 18% of eyes with the diffuse-trickling phenotype, raising the possibility that a subset of participants may have had an alternative underlying pathology.[33]

To mitigate this risk, we excluded eyes with GPS and patchy patterns and applied stringent criteria to identify and omit potential EMAP cases. Yet, pattern transitions were still observed, confirming that FAF evolution is a genuine feature of GA progression, even in a rigorously defined, AMD-specific cohort. Notably, in this cohort of strictly AMD-related GA, no transitions to diffuse-trickling patterns were observed, although such changes may occasionally occur, particularly in older patients with a high burden of reticular pseudodrusen.

Looking ahead, clinical trials may benefit from refining recruitment and monitoring strategies to account for the dynamic nature of FAF phenotypes. Eyes with early-stage patterns such as "none" or "focal" should not be categorically excluded, as they may still represent viable therapeutic windows where intervention could alter the disease course. Conversely, eyes presenting with diffuse-trickling features require careful scrutiny to avoid inadvertent inclusion of EMAP or allied retinal dystrophies. Incorporating longitudinal FAF imaging during study FU may also offer valuable insight into whether treatment modifies not only lesion enlargement but also the tempo or direction of phenotypic evolution. Post hoc subgroup analyses comparing treatment effects across evolving versus stable patterns, and across banded versus diffuse configurations, may further enhance our understanding of response heterogeneity.

Our study has several limitations. Its retrospective design and inclusion of only eyes with serial, gradable FAF imaging may introduce selection bias. Grading of the perilesional FAF pattern, while reproducible, remains a subjective task and might miss subtle or gradual transitions. Additionally, only visits flagged by the first grader were reviewed by the second, precluding formal assessment of interobserver reproducibility and potentially missing additional transitions. The inclusion of only foveal-sparing GA, while aligned with early-intervention goals and clinical trial eligibility criteria, limits generalizability, especially as recent evidence suggests that foveal-involving GA may be associated with comparable or greater functional decline.[34,35] Finally, in some cases, phenotypic change was first recognized at the last available FU, preventing assessment of posttransition dynamics. Nonetheless, our results carry both clinical and methodological implications, suggesting that reliance on baseline classification alone may oversimplify the complexity of GA.

In conclusion, our findings indicate that perilesional FAF patterns in GA are not static but can evolve. These transitions occur in a meaningful proportion of eyes, are associated with changes in lesion growth rate, and likely reflect broader structural and biological remodeling at the junctional zone. Importantly, baseline FAF phenotype did not predict visual acuity decline, suggesting limited functional prognostic value. As new therapies for GA emerge, incorporating longitudinal phenotypic assessment into clinical trials may improve stratification, enrich mechanistic understanding, and better capture meaningful treatment effects over time.

Declaration of Generative AI and AI-Assisted Technologies in the Writing Process

During the preparation of this work the authors used ChatGPT-4o in order to improve readability and language of the manuscript. After using this tool, the authors reviewed and edited the content as needed and take full responsibility for the content of the published article.

Footnotes and Disclosures

Originally received: June 23, 2025.
Final revision: October 9, 2025.
Accepted: October 29, 2025.
Available online: November 5, 2025. Manuscript no. XOPS-D-25-00439.

[1] Department of Ophthalmology, IRCCS San Raffaele Scientific Institute, Milan, Italy.

[2] School of Medicine, Vita-Salute San Raffaele University, Milan, Italy.

*A.A. and F.V. contributed equally as co-first authors.

Disclosure(s):

All authors have completed and submitted the ICMJE disclosures form.

The authors made the following disclosures:

M.B.P.: Consultant − Novartis.

F.B.: Consultant − Abbvie, Hoffmann-La-Roche, Adverum Biotechnologies Inc., Alimera Sciences, Apellis, Bayer Shering-Pharma, Boehringer-Ingelheim, Breye Therapeutics ApS, Fidia Sooft, Outlook Therapeutics, Novartis, NTC Pharma, Oxurion NV, 4D Molecular Therapeutics Inc., Sifi.

Support for Open Access publication was provided by IRCCS San Raffaele Scientific Institute.

HUMAN SUBJECTS: Human subjects were included in this study. The study protocol adhered to the Declaration of Helsinki and was exempted by the San Raffaele Hospital Institutional Review Board from the requirement for written informed consent.

No animal subjects were used in this study.

Author Contributions:

Conception and design: Cicinelli

Data collection: Antropoli, Vacirca, Introini, Bandello, Parodi

Analysis and interpretation: Antropoli, Vacirca, Parodi, Cicinelli

Obtained funding: N/A

Overall responsibility: Antropoli, Vacirca, Cicinelli

Abbreviations and Acronyms:
AMD = age-related macular degeneration; **BCVA** = best-corrected visual acuity; **CI** = confidence interval; **EMAP** = extensive macular atrophy with pseudodrusen-like appearance; **FAF** = fundus autofluorescence; **FU** = follow-up; **GA** = geographic atrophy; **GPS** = fine-granular with peripheral punctate spots; **IQR** = interquartile range; **RPE** = retinal pigment epithelium.

Keywords:
AMD, FAF pattern, Fundus autofluorescence, Geographic atrophy.

Correspondence:
Alessio Antropoli, MD, IRCCS San Raffaele Scientific Institute, Via Olgettina 60, Milan 20132, Italy. E-mail: antropoli.alessio@hsr.it.

References

1. Wong WL, Su X, Li X, et al. Global prevalence of age-related macular degeneration and disease burden projection for 2020 and 2040: a systematic review and meta-analysis. *Lancet Glob Health*. 2014;2:e106–e116.
2. Heier JS, Lad EM, Holz FG, et al. Pegcetacoplan for the treatment of geographic atrophy secondary to age-related macular degeneration (OAKS and DERBY): two multicentre, randomised, double-masked, sham-controlled, phase 3 trials. *Lancet*. 2023;402:1434–1448.
3. Khanani AM, Patel SS, Staurenghi G, et al. Efficacy and safety of avacincaptad pegol in patients with geographic atrophy (GATHER2): 12-month results from a randomised, double-masked, phase 3 trial. *Lancet*. 2023;402:1449–1458.
4. Csaky KG, Miller JML, Martin DF, Johnson MW. Drug approval for the treatment of geographic atrophy: how we got here and where we need to go. *Am J Ophthalmol*. 2024;263:231–239.
5. European Medicines Agency. Syfovre. 2024. https://www.ema.europa.eu/en/medicines/human/EPAR/syfovre. Accessed February 2, 2024
6. Bui PTA, Reiter GS, Fabianska M, et al. Fundus autofluorescence and optical coherence tomography biomarkers associated with the progression of geographic atrophy secondary to age-related macular degeneration. *Eye*. 2022;36:2013–2019.
7. Holmen IC, Aul B, Pak JW, et al. Precursors and development of geographic atrophy with autofluorescence imaging. *Ophthalmol Retina*. 2019;3:724–733.
8. Holz FG, Bindewald-Wittich A, Fleckenstein M, et al. Progression of geographic atrophy and impact of fundus autofluorescence patterns in age-related macular degeneration. *Am J Ophthalmol*. 2007;143:463–472.e2.
9. Shen LL, Liu F, Nardini HG, Del Priore LV. Reclassification of fundus autofluorescence patterns surrounding geographic atrophy based on progression rate: a systematic review and meta-analysis. *Retina*. 2019;39:1829–1839.
10. Teo KYC, Fujimoto S, Sadda SR, et al. Geographic atrophy phenotypes in subjects of different ethnicity. *Ophthalmol Retina*. 2023;7:593–604.
11. Fleckenstein M, Mitchell P, Freund KB, et al. The progression of geographic atrophy secondary to age-related macular degeneration. *Ophthalmology*. 2018;125:369–390.
12. Bindewald A. Classification of abnormal fundus autofluorescence patterns in the junctional zone of geographic atrophy in patients with age related macular degeneration. *Br J Ophthalmol*. 2005;89:874–878.
13. Smailhodzic D, Fleckenstein M, Theelen T, et al. Central Areolar Choroidal Dystrophy (CACD) and Age-Related Macular Degeneration (AMD): differentiating characteristics in multimodal imaging. *Invest Ophthalmol Vis Sci*. 2011;52:8908.
14. Lindner M, Lambertus S, Mauschitz MM, et al. Differential disease progression in atrophic age-related macular degeneration and late-onset stargardt disease. *Invest Ophthalmol Vis Sci*. 2017;58:1001.
15. Antropoli A, Arrigo A, Bianco L, et al. Quantitative multimodal imaging of extensive macular atrophy with pseudodrusen and geographic atrophy with diffuse trickling pattern. *Sci Rep*. 2023;13:1822.
16. Bianco L, Antropoli A, Arrigo A, et al. Fundus autofluorescence in extensive macular atrophy with pseudodrusen and diffuse trickling geographic atrophy. *Retina*. 2023;43:755.
17. Biarnés M, Arias L, Alonso J, et al. Increased fundus autofluorescence and progression of geographic atrophy secondary to age-related macular degeneration: the GAIN study. *Am J Ophthalmol*. 2015;160:345–353.e5.
18. Biarnés M, Monés J, Trindade F, et al. Intra and interobserver agreement in the classification of fundus autofluorescence patterns in geographic atrophy secondary to age-related macular degeneration. *Graefes Arch Clin Exp Ophthalmol*. 2012;250:485–490.
19. Biarnes M, Forero CG, Arias L, et al. Reappraisal of geographic atrophy patterns seen on fundus autofluorescence using a latent class analysis approach. *Invest Ophthalmol Vis Sci*. 2014;55:8302–8308.
20. Monés J, Biarnés M. Geographic atrophy phenotype identification by cluster analysis. *Br J Ophthalmol*. 2018;102:388–392.
21. Bearelly S, Khanifar AA, Lederer DE, et al. Use of fundus autofluorescence images to predict geographic atrophy progression. *Retina*. 2011;31:81–86.
22. Taha AT, Shen LL, Diaz A, et al. Association of hyperautofluorescence signals with geographic atrophy progression in the METformin for the MINimization of geographic atrophy progression trial. *Ophthalmol Sci*. 2025;5:100620.
23. Allingham MJ, Nie Q, Lad EM, et al. Semiautomatic segmentation of rim area focal hyperautofluorescence predicts progression of geographic atrophy due to dry age-related macular degeneration. *Invest Ophthalmol Vis Sci*. 2016;57:2283–2289.
24. Li AS, Myers J, Stinnett SS, et al. Gradeability and reproducibility of geographic atrophy measurement in GATHER-1, a phase II/III randomized interventional trial. *Ophthalmol Sci*. 2024;4:100383.
25. Cicinelli MV, Barlocci E, Giuffrè C, et al. Integrating machine learning and traditional survival analysis to identify key predictors of foveal involvement in geographic atrophy. *Invest Ophthalmol Vis Sci*. 2024;65:10.
26. Antropoli A, Bianco L, Romano F, et al. Extensive Macular Atrophy with Pseudodrusen-like appearance (EMAP) clinical characteristics, diagnostic criteria, and insights from allied Inherited retinal diseases and age-related macular degeneration. *Prog Retin Eye Res*. 2024;104:101320.
27. Holz FG, Sadda SR, Busbee B, et al. Efficacy and safety of lampalizumab for geographic atrophy due to age-related macular degeneration: chroma and spectri phase 3 randomized clinical trials. *JAMA Ophthalmol*. 2018;136:666–677.
28. Dreyhaupt J, Mansmann U, Pritsch M, et al. Modelling the natural history of geographic atrophy in patients with age-related macular degeneration. *Ophthalmic Epidemiol*. 2005;12:353–362.
29. Monés J, Biarnés M. The rate of progression of geographic atrophy decreases with increasing baseline lesion size even after the square root transformation. *Translational Vis Sci Technol*. 2018;7:40.
30. Antropoli A, Bianco L, Condroyer C, et al. Extensive Macular Atrophy with Pseudodrusen-like appearance (EMAP): progression kinetics and late-stage findings. *Ophthalmology*. 2024;131:1175–1184.

31. Romano F, Cozzi M, Monteduro D, et al. Natural course and classification of extensive macular atrophy with pseudodrusen-like appearance. *Retina*. 2023;43:402.
32. Romano F, Airaldi M, Cozzi M, et al. Progression of atrophy and visual outcomes in extensive macular atrophy with pseudodrusen-like appearance. *Ophthalmol Sci*. 2021;1:100016.
33. Patel SS, Lally DR, Hsu J, et al. Avacincaptad pegol for geographic atrophy secondary to age-related macular degeneration: 18-month findings from the GATHER1 trial. *Eye (Lond)*. 2023;37:3551−3557.
34. Anegondi N, Steffen V, Sadda SR, et al. Visual loss in geographic atrophy: learnings from the lampalizumab trials. *Ophthalmology*. 2025;132:420−430.
35. Shen LL, Kaiser PK, Liu J, et al. Determinants of four-year visual acuity loss in geographic atrophy: an analysis of age-related eye disease study and age-related eye disease study 2. *Ophthalmology*. 2025;132:785−798.